RSC Advances

PAPER

View Article Online
View Journal | View Issue

Cite this: *RSC Adv.*, 2025, **15**, 25473

A hybrid acoustofluidic device with Parafilm® that operates as a traditional bulk acoustic wave or flexural plate wave device†

Abelino Vargas Jiménez, *[abc] Diana Carolina Ochoa Cabezas, [abd] Michael Delay, [e] Itziar González Gómez [f] and Marcela Camacho [a]

Received 4th April 2025
Accepted 30th June 2025

DOI: 10.1039/d5ra02351c

rsc.li/rsc-advances

In this article we describe new hybrid microfluidic acoustic devices (HMADs) composed of two types of materials: soft elastic lateral walls made of Parafilm® that include a channel, and rigid top and bottom walls consisting of a glass slide and a glass coverslip. Depending on the selected vibration frequency of two small piezoelectric transducers, these HMADs can operate as Bulk Acoustic Wave (BAW) or as Flexural Plate Wave (FPW) devices, which induce either levitating circular or linear particle aggregates at higher frequencies when operating as BAW-like devices, or at acoustic frequencies close to those of the transducer's thickness mode when operating as FPW-like devices. The use of a soft, elastic material permits a range of different geometrical channel configurations. These HMADs in the BAW-like mode induce the formation of very stable aggregates, and in the FPW-like mode allow manipulation and control of the position or angular motion of particles and cells with micrometric precision when a phase change is induced between the two transducers.

1 Introduction

During recent decades, special interest has arisen in lab-on-a-chip platforms and microfluidic devices for the study and manipulation of liquid samples. Diverse studies in the literature describe developments of active microfluidic systems, in which acoustic fields in the ultrasound range are used to manipulate particles or cells for various environmental and biomedical applications, among others. In these approaches, different materials and techniques are used to build microfluidic acoustic devices (MADs) for cell manipulation and/or separation, based on transmission of Bulk Acoustic Waves (BAW) or Surface Acoustic Waves (SAW).

Traditional BAW devices are made up of rigid constitutive materials to maximize reflection of the acoustic waves at the channel walls, which is necessary to establish standing waves in the contained liquid sample. Materials with high acoustic impedance such as glass, silicon, or stainless steel and channels with simple geometries are generally used for BAW devices.

In contrast, the SAW configuration employs interference of ultrasonic waves propagating on the surface of a piezoelectric substrate.[1,2] These devices propagate the acoustic waves within a channel layered on the piezoelectric substrate, do not require special rigidity or other characteristics, allow the use of materials with low acoustic impedance such as the polymer polydimethylsiloxane (PDMS)[3,4] which is easy to manipulate mechanically, and enable MADs with complex geometries.[5,6]

Despite advances in manufacturing techniques of MADs using different materials, the access to this technology and its commercialization remains limited.[1] This is partly due to production requirements for clean room facilities and lithographic technology. In addition, BAW devices require rigid materials that are difficult to process and slow to manufacture,[7] while SAW devices use interdigital transducers (IDTs).[1] Efforts have been made in the last decade to build more accessible BAW devices using micro glass capillaries of square rectangular section for diverse applications,[8–10] but their use is limited because their geometry cannot be modified.

BAW devices have since been based on polymeric materials,[6,11–13] but these develop very complex three-dimensional vibration patterns across the chip, whose acoustic pressure patterns in the containment channel are unstable over a variation of a few Hz. These structural vibration modes depend on the whole device geometry, acoustic wave frequency, and physical properties of the material used in its construction. The observed modes are difficult to identify

[a]*Laboratorio de Biofísica, Departamento de Biología, Facultad de Ciencias, Universidad Nacional de Colombia, Bogotá, Colombia. E-mail: avargasj@unal.edu.co*
[b]*Centro Internacional de Física (CIF), Bogotá, Colombia*
[c]*Universidad Pedagógica Nacional, Departamento de Biología, Bogotá, Colombia*
[d]*Universidad de la Salle, Departamento de Biología, Bogotá, Colombia*
[e]*IDEX Health & Science, Rochester, New York, USA*
[f]*Concejo Superior de Investigaciones Científicas (CSIC), Instituto de Tecnologías Físicas y de la Información (ITEFI), Madrid, Spain*

† Electronic supplementary information (ESI) available. See DOI: https://doi.org/10.1039/d5ra02351c

theoretically, leaving numerical analysis as the only tool to predict the behavior and to allow optimization of their use in the separation or handling of cells.[11,12,14]

A third type of ultrasonic actuation was described for the "THINUS" chip,[15] whose mode of operation is intermediate between BAW and SAW. In these devices, the radiation force arises from complex acoustic pressure patterns established in the liquid phase of the channel and transmitted through the liquid–solid interface from three-dimensional vibrations generated across the chip structure. The larger the chip surface area to thickness ratio, the closer the vibrations are to those of a plate. These acoustic fields are transferred to the liquid sample circulating through the microfluidic channel and can position small particles in one or two dimensions and keep them in an equilibrium position in the third dimension. By changing the sound field, it is possible to propel the particles in a controlled manner. The design is based on a very large surface/volume ratio configuration with a polymeric structure, which provides a vibrating plate-like actuation at different specific frequencies in an scalable manner. The chip itself is made from a rectangular sheet of SU-8 epoxy formed with channel structures and layered on a thicker substrate of the same material. This configuration allows the establishment of two-dimensional resonances throughout the chip structure along the very thin direction transverse to its thickness, resulting in the chip behaving as a rectangular plate with flexural vibrations.

More recently, another type of acoustic device that uses Lamb waves has been developed, referred to as a Flexural Plate Wave (FPW), which usually operates at frequencies between 5 and 20 MHz, lower than the frequencies used in traditional SAW devices.[15,16] Its construction can use low or high acoustic impedance materials, along with piezoelectric ceramic transducers or IDTs. Recently a FPW device was built using silicon and aluminum nitrate as constituent materials of the flexural plate, coupled to two opposing IDTs located on the bottom of the device, so as to cluster and align microparticles after complete evaporation of a water droplet.[16]

An approach to make acoustic lab-on-a-chip platforms more versatile and accessible uses low cost commercial materials in the MADs and non-acoustic microfluidic devices. Strips of aluminum foil pressed onto piezoelectric substrates allow generation of Lamb waves of amplitude sufficient to transport, manipulate, microcentrifuge and nebulize sessile drops and paper in 3D configurations.[17] In another example, Parafilm was machine-cut into geometrical patterns with sharp angular distributions tolerant to different pH values and some polar solvents, with the resulting device acting as a two-dimensional concentration gradient generator and microfluidic electrochemical transducer. Parafilm was found advantageous in the construction of non-acoustic microfluidic devices as it is a thermoplastic material with a low melting point that allows a strong union between the plates with little deformation of the microchannel when using a sealing temperature of 55 °C and pressure of 0.13 MPa.[18]

Our research groups described a hybrid acoustic device, in which aluminum sheets with channels were located on a rectangular microscope glass slide. The device acts as a thick vibrating plate due to the acoustic actuation by a ceramic piezoelectric transducer attached underneath.[19] Other more sophisticated hybrid resonators were later developed to collect particles or cells; these used extremely soft materials, such as water-based gels as the upper channelized medium, with the flowing liquid suspension layered on a rigid substrate.[20]

This trend towards using unconventional materials in HMADs construction has resulted in new chip configurations offering novel advantages, simpler designs, ease of manufacture without need for a clean room or lithographic technology, and portability for field work. Some of these have been shown to be efficient in specific biomedical applications.[7,20] These technologies open the door to a new generation of economical, versatile, and mechanically robust HMADs that can be employed for many different applications.

A new type of HMAD is reported here which can operate as a BAW or FPW device, depending on the selected frequency. It consists of a thin Parafilm sheet, on which the channel is cut, held between a microscope glass slide and a glass cover slip that acts as the substrate. The system is acoustophoretically actuated by two facing PZ26 piezoelectric transducers attached under the glass cover slip. In the following sections we describe the construction process and the experimental procedures used to identify the specific frequencies at which these devices operate in either BAW-like or FPW-like mode.

2 Methods and materials

The device shown in this work is composed of two small piezoelectric transducers, a microscope glass slide, a Parafilm layer into which the channel is cut, and a glass coverslip that keeps the channeled Parafilm layer sandwiched between the two glass plates (Fig. 1). The ultrasonic transducers are coupled either in parallel or perpendicular to each other on the HMADs (Fig. 2) to induce BAW-like or FPW-like operation modes, allowing stable spherical aggregates and the manipulation of the lateral position of particles or cells by changing the phase difference between the two transducers.

2.1 Acoustic device and experimental setup

In the HMADs used in this work, particle or cell samples were suspended in a liquid medium exposed to ultrasonic waves. The sample flow was controlled by pumps (Pump 33 DDS, KD Scientific, Harvard Apparatus, Holliston, MA, USA) connected to their inlets and outlets. The ultrasonic waves in the HMADs were generated by two PZ26 piezoelectric ceramic actuators with a thickness-mode resonance at 2 or 5 MHz (Ferroperm™ Piezoceramics, Meggitt A/S, Kvistgard, Denmark) with rectangular geometry and small dimensions of 15 mm × 4 mm that vibrated simultaneously at the same frequency in the thickness direction of the channel.

A glass slide and a thin rectangular or square glass coverslip of standard thickness were used (Fig. 1b and 2). The inlets and outlets in the HMADs were formed on the slide using a rotary tool (Dremel 395, Mount Prospect, IL, USA) with a 1 mm

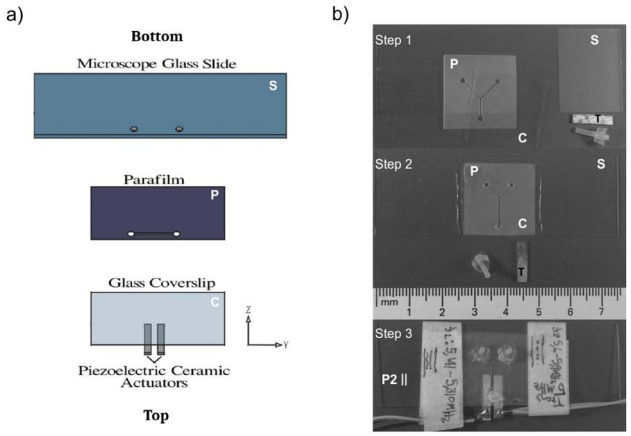

Fig. 1 HMAD build process. (a) Building materials and location of the glass slide (S), Parafilm sheet (P), glass coverslip (C), and PZ26 piezoelectric ceramic actuators (T) in the construction process; (b) steps of the construction process: step 1 building materials, step 2 joining of S and C with the Parafilm after thermal treatment and step 3 attaching the transducers to the device and adjusting the input and output. The words top and bottom indicate the location of the HMADs when they were placed under the microscope.

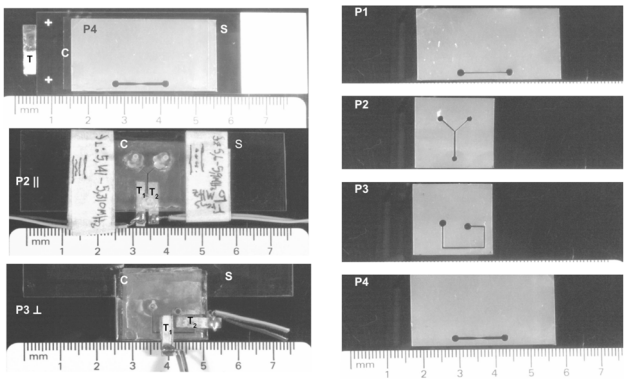

Fig. 2 Location of the piezoelectric transducers in the HMADs: P|| parallel or P⊥ perpendicular configurations; and geometries P1, P2, P3 and P4 cut in the Parafilm.

diameter diamond drill bit (Drilax X000XA0F53, Warren, NJ, USA) and a biocompatible tube of 1.5 mm diameter (Fig. 1b). As the Parafilm is elastic, the channels were cut using a cutting plotter (Graphtec CE6000-60 PLUS, Graphtec America, Irvine, CA, USA) with a blade of 0.899 mm (Graphtec CB09UB) to generate different geometries, which were designed using the FreeCAD software, version 0.15 (**https://www.freecad.org**). The Parafilm sheet with the channel was cut to the same lateral dimensions as the coverslip (Fig. 2 P1–4).

The HMADs were formed by sandwiching the low acoustic impedance material, *i.e.*, the Parafilm sheet with the channel, between the high acoustic impedance material, *i.e.* the glass plates (Fig. 1). Once in place, the Parafilm was pressed upon by the glass substrate and subjected for five minutes to 55 ± 1 °C to improve its adherent properties. The seal was completed with epoxy glue deposited along the edges of the coverslip. The two piezoelectric ceramic actuators were then coupled to the device on the glass coverslip (Fig. 1b), because the resonance improved if the transducers were on the thinner glass plate. These transducers could be located parallel (Fig. 2 P2||) or perpendicular to each other (Fig. 2 P3⊥), and parallel (Fig. 2 P2||; Fig. 2 P3 ⊥ T_2) or perpendicular (Fig. 2 P3 ⊥ T_1) to the position of the channel.

The final dimensions of the channels inside the HMADs were measured using an Olympus BXM15M reflection microscope (Olympus Corp., Tokyo, Japan) with Olympus Stream Basic 1.9 Software that had been spatially calibrated. The dimensions of the hybrid devices can be reviewed in the ESI.†

The acoustic field was created by two ceramic actuators driven by a 10 V peak-to-peak signal from a two-channel waveform generator (AFG3102C, Tektronix Inc., Beaverton, OR, USA) at the same frequency to establish the resonance in the device. Due to the thickness of the glass coverslip and the two piezoelectric transducers that vibrate at the same frequency simultaneously, the acoustic experiments could be carried out without a power amplifier. Finally, the images and video recordings of the motion of the different samples inside the HMADs were obtained by BX51M reflection microscopy with an Olympus SC100 digital camera connected to a computer running Olympus Stream Basic 1.9 software.

2.2 Sample preparation

To identify the main resonance modes in the HMADs, suspensions of particles were prepared using polystyrene beads (Polybead Microspheres, Polysciences, Inc., Warrington, PA, USA) of diameters 4.5 and 10.0 μm. 100.0 or 150.0 μL of these particles were diluted in 1 mL of deionized and distilled water to obtain different concentrations. After finding the main resonance modes with these samples, 1 mL of the different biological samples were used in the acoustic experiments.

The biological samples were cells with a concentration of (~0.4×10^6 cells per mL), assumed spherical in suspension, of the breast cancer cell line MCF-7 (ATCC HTB-22) or the cervical cancer SiHa line (ATCC HTB-35), cultured at 37 ± 1 °C and 5% CO_2 in 25 cm^2 flasks in RPMI (ThermoFisher, Waltham, MA, USA) supplemented with 10% heat inactivated fetal bovine serum (FBS CVFSVF00-01 eurobio scientific) and kept at 7.4 pH. Cells were passed upon reaching 80% confluence (~1×10^6 cells per mL) by enzymatic treatment with 1 mL of 1% trypsin-EDTA solution (Trypsin-Versene (EDTA) Mixture (1X), Lonza, Basel, Switzerland).

A smaller non-spherical and mobile cell was also explored. *Leishmania panamensis* promastigotes, a protozoan parasite of relevance to public health, isolate HOM/PA/71/LS94, kindly donated by the Centro Internacional de Entrenamiento e Investigaciones Médicas (CIDEIM, Cali, Colombia), were cultured at 26 ± 1 °C in 25 cm^2 completely closed flasks in 10 mL of Schneider's Insect Medium (ThermoFisher, Waltham, MA, USA) supplemented with 10% FBS at pH 7.4. To maintain this parasite state, approximately half of the culture was removed and replaced by fresh medium when the promastigote culture reached 95% (~2×10^6 cells per mL). Dead parasites were removed by gravitational sedimentation at 1 g.

Table 1 Characterization of the resonance frequencies of HMADs

HMAD	Channel geometry	Transducers position	Piezoelectric transducers frequency (MHz)	HMAD experimental resonance frequency (MHz)	Theoretical and electrical characterization acoustic resonance (MHz)	Q (FPW-like mode)
P1‖	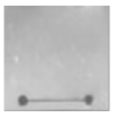	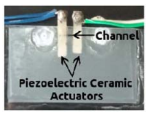	5	BAW-like mode: 5.834 FPW-like mode: 5.443	BAW-like mode: 5.704 eqn (1) FPW-like mode: 5.134 Fig. 6a	15.6
			2	FPW-like mode: 1.872	FPW-like mode: 1.872 Fig. 6b	8.2
P2‖		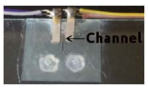	5	BAW-like mode: 5.900 FPW-like mode: 5.141	BAW-like mode: 5.704 eqn (1) FPW-like mode: —	—
			2	FPW-like mode: 2.019	FPW-like mode: 1.950 Fig. 6c	10.7
P3 ⊥	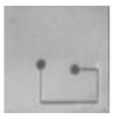		5	BAW-like mode: unidentified FPW-like mode: 4.901/3.275	BAW-like mode: 5.704 eqn (1) FPW-like mode: 4.908 Fig. 6d	9.8
			2	FPW-like mode: 2.141	FPW-like mode: —	—
P4‖	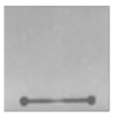		5	BAW-like mode: 5.810 FPW-like mode: 5.337	BAW-like mode: 5.704 eqn (1) FPW-like mode: —	—
			2	FPW-like mode: 1.790	FPW-like mode: —	—

3 Results and discussion

3.1 HMADs device resonance modes in P‖ configuration

The acoustic tests revealed two main resonance modes of interest in the different HMADs built (Table 1), when the two piezoelectric ceramic actuators of 2 or 5 MHz, located in parallel, were driven at the same frequency (Fig. 3 and 4).

The BAW-like mode was established in HMADs coupled to 5 MHz transducers for experimental resonance frequencies close to 5.8 MHz, at which the formation of very stable circular aggregates was observed (Fig. 3 and Video 1†). To explain the formation of these aggregates, it can be assumed that the acoustic waves generated by the transducers are reflected between the rigid walls of the channel defined by the glass

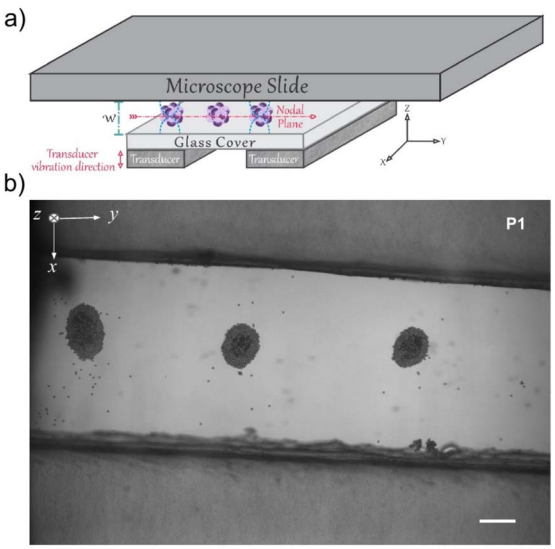

Fig. 3 HMAD in BAW-like mode. (a) Explanatory diagram of the BAW-like mode generated by the reflection of waves between the glass slide and the glass coverslip. Here w corresponds to the thickness of the Parafilm; (b) circular aggregates formed in BAW-like mode in an HMAD built with Parafilm sheet P1 and two transducers at 5 MHz located in parallel, obtained at the frequency 5.834 MHz with microparticles of 4.5 μm diameter. Scale bar ~100 μm.

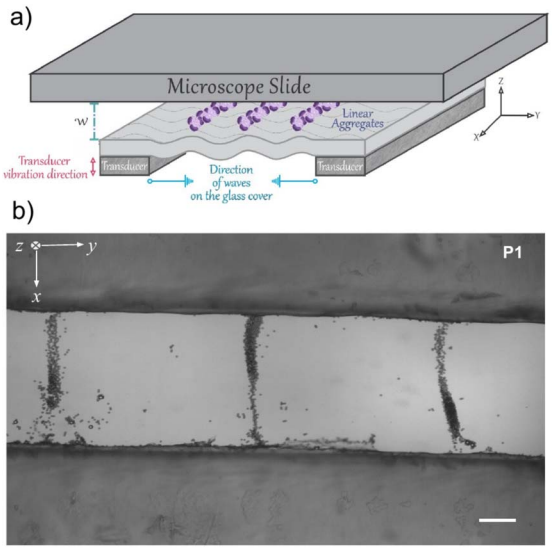

Fig. 4 HMAD in FPW-like mode. (a) Explanatory diagram of the FPW-like mode generated by the interference of Lamb waves propagating on the glass coverslip in opposite directions. Here w corresponds to the thickness of the Parafilm; (b) linear aggregates formed in a HMAD built with a Parafilm sheet P1 and two transducers at 2 MHz located in parallel, obtained at the frequency 1.872 MHz with microparticles of 4.5 μm diameter. Scale bar ~100 μm.

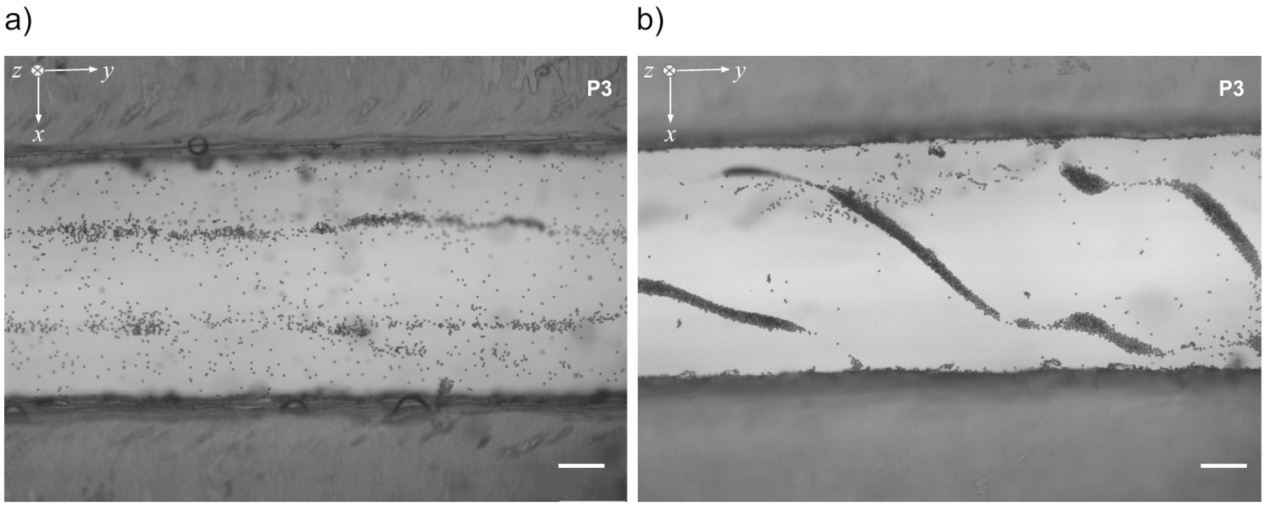

Fig. 5 Aggregates formed by microparticles of 4.5 μm diameter in the HMADs using two transducers of 5 MHz oriented perpendicularly with the P3 geometry. (a) Two parallel linear aggregates for an experimental frequency 4.901 MHz, and (b) diagonal aggregate for an experimental frequency of 3.275 MHz. Scale bars ~100 μm.

coverslip and the glass slide to induce a standing wave interference pattern with a nodal plane in the center of the device (Fig. 3a). In this mode, the HMAD operates as a traditional BAW device in which standing waves are generated by the interference of reflected waves between the rigid walls of the resonant cavity.[1,4,11] In this case, the resonant frequency can be calculated

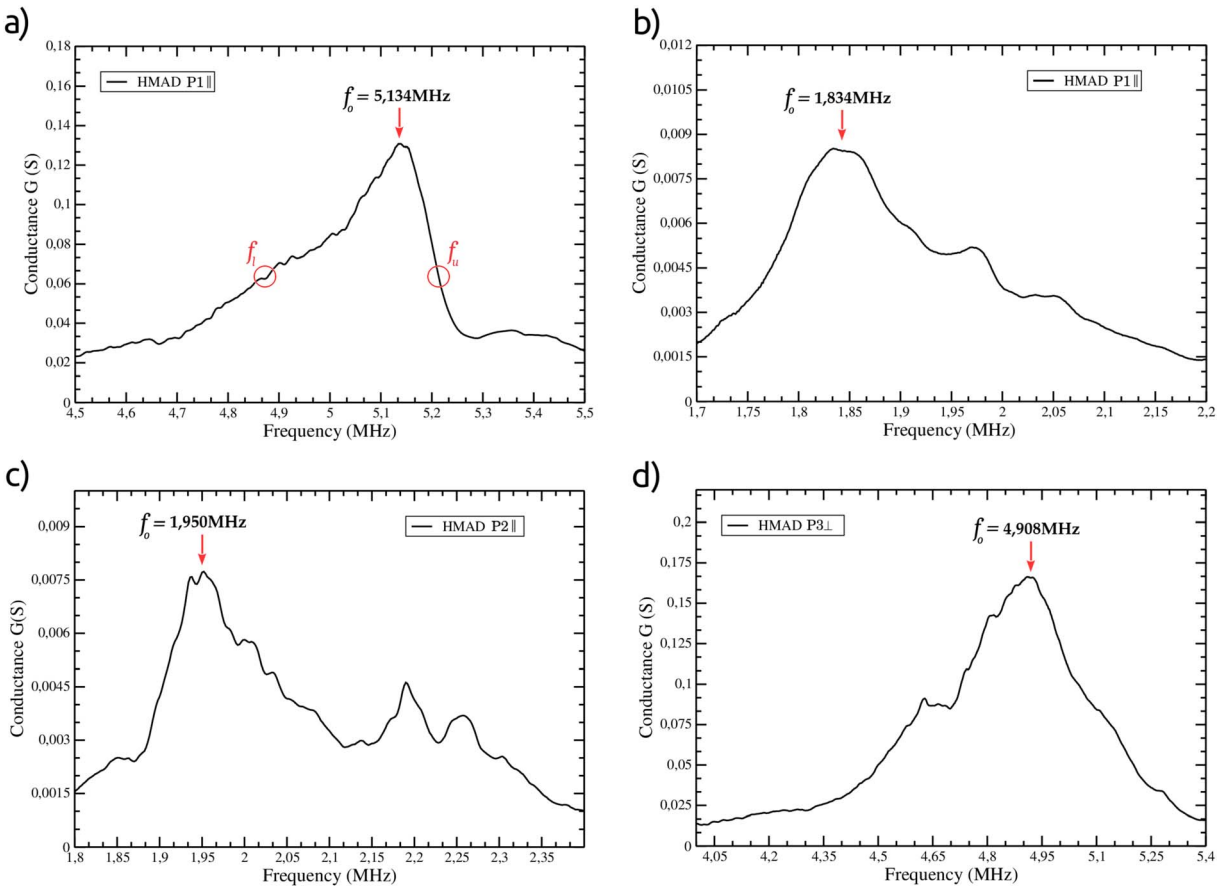

Fig. 6 Measurements of electrical conductance G of the HMADs coupled to two piezoelectric transducers. In (a and b) the electrical response (HMAD P1∥ geometry) is shown, when the device is attached to two piezoelectric ceramic actuators of 5 MHz or 2 MHz respectively. (c) Electrical response of a HMAD with P2∥ geometry coupled to transducers of 2 MHz; and (d) electrical characterization of a HMAD with P3⊥ geometry attached to transducers of 5 MHz.

from the thickness of the Parafilm ($w \cong 130$ μm), assuming that a pressure node is established in the z direction at the center of the channel for a resonance condition of $\lambda/2$ (Fig. 3a). The unidimensional expression for the resonance frequency is then

$$f_o = \frac{c_o}{2w} = 5.704 \text{ MHz} \quad (1)$$

where c_o is the sound velocity in the liquid medium, 1483 m s^{-1}. The theoretical resonance frequency defined by eqn (1) is near the value 5.834 MHz identified experimentally in the HMAD P1 coupled to 5 MHz transducers (Table 1 and Fig. 3b). The difference between these frequency values may be accounted for by changes in the Parafilm thickness during the construction process, as the heat and pressure applied can vary.

The FPW-like mode is established by the interference of waves propagating in opposite directions on the glass coverslip (Fig. 4a). In this mode, linear aggregates form parallel to the position of the transducers when the resonance frequency of the device is near the vibration frequency of the piezoelectric transducers (see Fig. 4b and Video 2†). The wave interference generates a standing wave acoustic field on the glass coverslip that is transmitted to the fluid with the sample near the thin glass plate in the form of compressional acoustic waves. This field exerts an acoustic radiation force on the sample suspended in the liquid that forms parallel linear aggregates at the pressure nodes of the standing wave (Fig. 4). It should be pointed out that the operating principle to establish interference is similar to that used in conventional SAW devices, where the manipulation of particles or cells is performed with a stationary acoustic field generated by the superposition of two surface acoustic waves that propagate in opposite directions through the solid–liquid interface at a piezoelectric substrate.[1,4,11] Because the thicknesses of the transducers and the glass coverslip are in the same range this thin glass plate is deformed, generating Lamb waves in the HMADs shown here, as opposed to Rayleigh waves that propagate on the surface of an standard SAW device. In the FPW-like mode, the waves propagate in the entire volume of the glass coverslip perpendicularly to the direction of its deformation (Fig. 4), establishing vibration modes on this glass plate that can be symmetric or antisymmetric as described previously.[21–23]

It is important to note that the resonance modes reported here were identified in all HMADs built with transducers placed in parallel. In particular, the resonance frequency in the BAW-like mode was similar in all devices in which measurements were made, ranging between 5.750 and 5.900 MHz (Table 1) and frequencies in the FPW-like mode close to the vibration frequency of the transducers (Table 1).

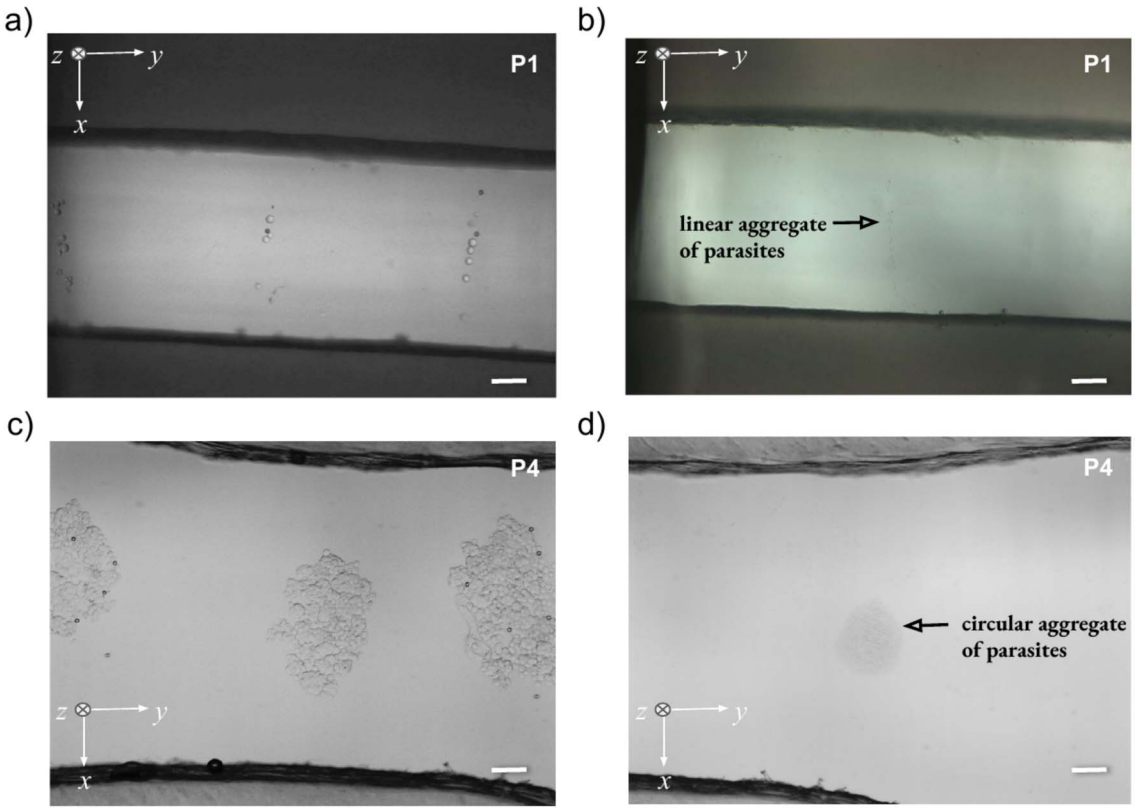

Fig. 7 Aggregates formed by different cell populations in both resonance modes inside HMADs. (a and b) Show linear aggregates formed by the cervical cancer line SiHa and *L. panamensis* promastigotes, respectively, in the FPW-like resonance mode for an experimental frequency of 1.873 MHz in the HMAD P1‖ attached to 2 MHz transducers. (c and d) Show circular aggregates formed by cells of the breast cancer line MCF-7 and *L. panamensis* promastigotes, respectively, in the BAW-like resonance mode using an experimental frequency of 5.810 MHz in the HMAD P4‖ attached to 5 MHz transducers. Scale bars ~100 μm.

3.2 HMADs device resonance modes in P⊥ configuration

Additional and more complex resonance modes were observed in the HMADs with P3 geometry, where the transducers were arranged perpendicularly (Table 1 and Fig. 2 P3⊥). In the case of the 5 MHz transducers, two different aggregates formed: one parallel to the channel walls, at a frequency close to the vibration frequency of the transducers (Fig. 5a), and another diagonal (Fig. 5b) at a lower frequency. For 2 MHz transducers, only diagonal linear aggregates were observed, similar to those shown in Fig. 5b, at an imposed frequency of 2.141 MHz, near the vibration frequency of the transducers.

It is important to highlight that the linear aggregates obtained in the perpendicular configuration of the transducers (2 or 5 MHz) can be associated with the FPW-like mode and the experimental resonance frequencies found, which have values close to the vibration frequencies of the transducers as shown in Table 1, HMAD P3⊥. Moreover, in the perpendicular configuration of the transducers for frequencies close to 5.8 MHz, the circular aggregate formation was not observed, which suggests that the BAW-like mode is not induced. We may suppose therefore that the BAW-like mode does not depend only on the reflection of the waves between the glass slide and coverslip in the z direction, but may involve a more complex mechanism, in which the waves generated in the (x, y) plane on the coverslip and the Parafilm also participate.

As the form and location of the aggregates generated in the HMADs shown in Fig. 3–5 are different, it is concluded that the pressure field inside the channel changes according to the transducer orientation, *i.e.* parallel *vs.* perpendicular. However, the aggregates shown in Fig. 5 were difficult to reproduce and in addition were unstable, suggesting that the acoustic equilibrium zones inside the HMADs with the perpendicular configuration of the transducers require further analysis to understand practical applications.

3.3 Electrical behavior of the HMAD

The electrical responses of some HMADs were studied to obtain information on their resonance modes in a non-destructive characterization using admittance data. The electrical conductance in the piezoelectric ceramics was monitored by an HP 4192A Impedance Analyzer (Hewlett-Packard, Palo Alto, CA, USA). For three selected HMADs, well-defined peaks are seen at specific frequencies (Fig. 6, red arrows) that correspond to values close to the resonance frequencies found experimentally with particles in the FPW-like resonance mode during the formation of linear aggregates. Table 1 summarizes these frequencies and those at which aggregation was observed. It should be noted that in this electrical characterization no higher resonance frequencies close to the BAW-like resonance mode were identified.

Based on the electrical conductance G data (Fig. 6), the quality factor Q related with the FPW-like resonance mode was estimated (Table 1) and the upper and a lower frequencies f_u and f_l at which the maximum conductance reaches half of its

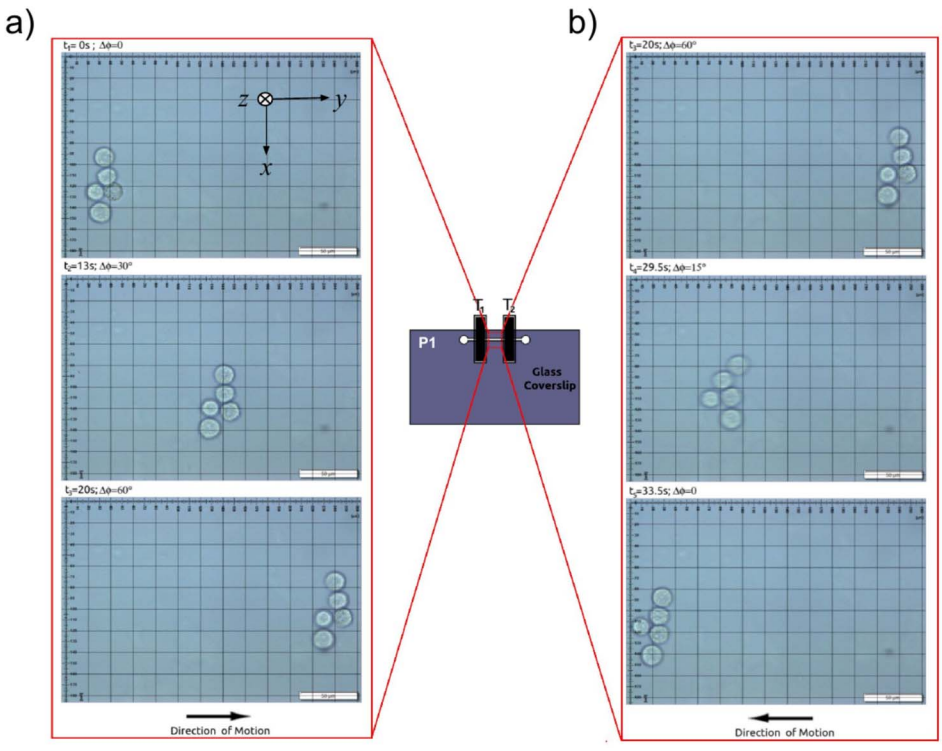

Fig. 8 Position manipulation of an aggregate of SiHa cells in HMAD P1|| in the FPW-like resonance mode due to a phase change in the acoustic wave generated by transducer 1 (T_1). (a) Movement of the aggregate toward the right when increasing the phase difference between the transducers; and (b) movement of the aggregate toward the left when decreasing the phase difference between the transducers. Resonance was obtained with piezoelectric ceramic actuators of 2 MHz at frequency 1.873 MHz.

value were identified. With the values f_u and f_l, the bandwidth $\Delta f = f_u - f_l$ was determined to find the Q factor when dividing the resonance frequency f_o by Δf.[24]

The Q factor of the HMADs in FPW-like mode presented here varies between 8 and 16 for resonant frequencies in the range of 1 to 6 MHz (Table 1). We note that the Q factor values reported in different acoustofluidic devices are quite variable, as this parameter measures the efficiency with which a resonant system stores and dissipates energy. Under low damping conditions, there is little energy dissipation and Q is high, and conversely under high damping conditions more energy is dissipated, resulting in a low Q. The Q value is seen to be affected by the device design, the materials used in its construction, and the operating conditions.

The Q values for the HMADs studied here are low, which may be due to the low acoustic impedance of Parafilm, an elastic material that absorbs a large part of the acoustic energy issued by the transducers. Furthermore, the dimensions of the Parafilm and the glass slide increase the mass loading of the HMADs, which are considered passive elements of the system, unlike the transducers. The gain of the piezoelectric ceramic actuators therefore decreases, reducing Q. In any case, the Parafilm HMADs require only small amount of low electrical power for their operation, and the supply voltage of the transducers can be increased using a power amplifier or, in our case, implementing a dual transducer system to minimize degradation of performance.

3.4 Acoustic manipulation and control of cells

Different HMAD transducer positions were chosen to study the dynamics of particles or cells exposed to the acoustic field (Table 1). Cell shape and size acted as differential parameters in the generation of stable aggregates (Fig. 7) for both operational modes. For example, levitation in linear aggregates (2D) results when the FPW-like resonance mode is imposed (Fig. 7a, b; and Videos 3, 4†), whereas circular aggregates (2D) are formed in the resonance BAW-like mode (Fig. 7c, d; and Videos 5, 6†), which are very stable in time despite the presence of flow established inside the channel.

The acoustophoretic motion of both cancer cell lines studied is similar to that observed in experiments with particles of diameter 4.5 and 10.0 μm, indicating that shape is important; note that these cells tend to be spherical in suspension. Because of their shape and size, 15 to 20 μm diameter, the radiation force is the main acoustic force that moves the cells towards the pressure nodes in the acoustic standing waves formed in both resonance modes described (Fig. 7a, c; and Videos 3, 5†).

Leishmania promastigotes are elongated, mobile, and have only about 10% of the volume[8] of the particles or cells studied here. The small volume is expected to result in a significantly reduced acoustic radiation force, which is directly proportional to volume.[8] In addition, the acoustophoretic motion of promastigotes towards the pressure node depends on their initial angular position since the parasite experiences an acoustic torque due to their elongated shape that generates rotational movement while being driven towards the pressure node.[8]

Although the initial angular positions of *Leishmania* promastigotes are important for its acoustophoretic motion, unlike that of the cells previously described, the parasites also form aggregates in both operational HMAD resonance modes (Fig. 7b, d; and Videos 4, 6†). However, with their small volume and elongated shape, their acoustophoretic motion is strongly influenced by the drag force induced by the acoustic streaming which results in longer aggregation times and a less orderly motion of the parasites towards the pressure node (Videos 4 and 6†).

Changing the phase between the piezoelectric ceramic actuators in the FPW-like resonance mode allowed control and manipulation of particles and the different cells used in this study (Fig. 8 and Videos 7, 8†). This appears to be proportional to the phase, as the increase or decrease of $\pi/6$ radians in the phase between the waves induces changes in position of the cellular aggregates of approximately 30 μm to the right (Fig. 8a) or to the left respectively (Fig. 8b). Similarly, microparticles of 10 μm diameter move between the two transducers upon changes in the phase difference (Video 8 and Fig. 5 of ESI†); the linear aggregates in the HMAD P2∥ (Table 1) move 50 μm towards the right for a phase variation of $5\pi/6$ radians if only the T_1 phase is modified, and to the left by the same distance if the T_1 phase is changed (Fig. 6 of ESI†).

In HMAD P3⊥ (Table 1), the phase difference between the two acoustic waves resulted in a rotatory motion in the FPW-like

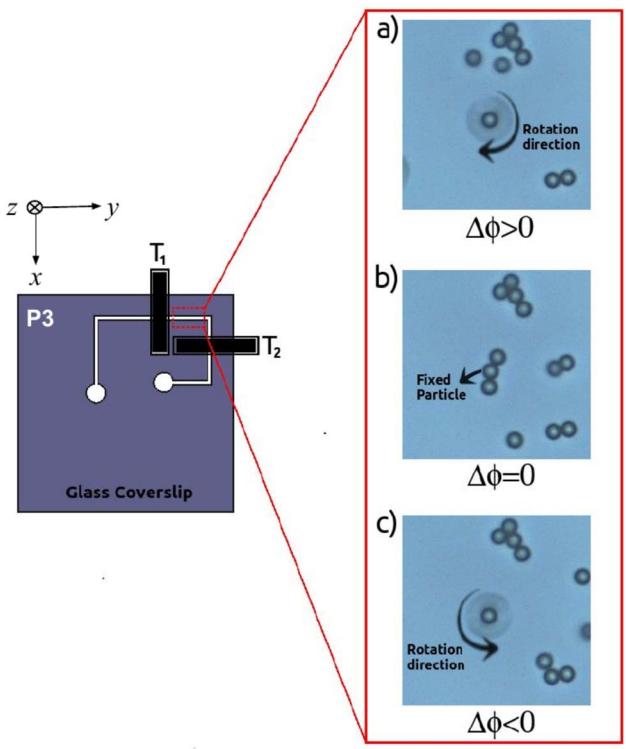

Fig. 9 Microparticle rotational motion in the HMAD P3⊥ coupled with 2 MHz piezoelectric ceramic actuators at resonance frequency 1.818 MHz. (a) 4.5 μm particles rotating clockwise around a fixed particle under a positive phase difference; (b) non-rotating particles under zero phase difference; and (c) particles rotating counterclockwise under a negative phase difference.

mode (Fig. 9 and Video 9†). If the phase difference between the waves generated by the transducers was larger than zero, the particle's direction of rotation was clockwise (Fig. 9a), with two latex microparticles of 4.5 μm diameter rotating around a fixed particle. When there was no phase difference between the waves, no rotational movement was established in the microparticles (Fig. 9b), and when the phase difference between the waves was less than zero, the particle's direction of rotation was counterclockwise (Fig. 9c). The angular velocity varied depending on the phase difference, increasing when large and decreasing when small, respectively. This dependence of the rotation rate of microparticles or cells on the phase difference is consistent with this phase difference causing a change in the acoustic streaming pattern around the particles.

4 Conclusions

In this paper we present a method for easy, low-cost construction of HMADs that can be used in laboratories with no clean room facilities or lithographic technology, and is portable for field or classroom use. These devices can be used in undergraduate Biophysics laboratories to demonstrate basic principles of acoustofluidics in the manipulation and sorting of particles or cells. It is also possible to study cell adhesion or aggregation, and to build model tissues, as previously described using a similar device.[25]

The HMADs are operationally flexible, as was identified experimentally due to their adaptability to either BAW-like or FPW-like devices, depending on the selected vibration frequency, which permits one to conceive of its use in varied applications. They show high frequency versatility and can be simply manufactured as described above. The choice of Parafilm in this implementation is a key step that allows for rapid construction of multiple channels with different desired geometries depending on the application (Fig. 2 and Table 1). The soft elastic thermoplastic material has been used as structural material in microfluidic devices,[18,26–29] where it is noted that its properties of hydrophobicity, softness, and adhesion at low temperatures make it an attractive material. In addition, due to the low melting point, HMADs and other MADs built with this material can be fabricated without the need for glue in the channel.[18,26,27]

Although Parafilm has low acoustic impedance, its softness and elasticity can interfere with the establishment of standing waves in the liquid phase contained between the walls of the channel. However, the HMADs presented here demonstrate well-defined resonance modes that allow aggregation and/or manipulation of particles and different cell types, when two small rectangular PZ26 transducers are used in parallel or perpendicular configuration.

The manipulation of particles or cells in HMADs (Fig. 8 and 9) can be relevant to basic and clinical work, since controlling the positions of the aggregates by phase change may improve our capability to separate and isolate these materials. In addition, manipulating position and/or rotational orientation of single cells potentially allows measurement of cell mechanical properties, such as elasticity or density, which may be important as they can be used in the differential diagnosis of pathologies such as cancer,[30] malaria,[31] or SARS-CoV-2.[32]

Finally, it is shown that manipulation of particles and cells with different shape and mobility with micrometric precision is achieved in these hybrid devices by varying the phase between the piezoelectric ceramic actuators. The BAW-like mode additionally allows the formation of stable aggregates despite the flow of the liquid medium, and the FPW-mode permits precise manipulation and control of position and rotation of the particles or cells.

Data availability

Data for this article, images and videos, have been included as part of the ESI.†

Author contributions

Abelino Vargas Jiménez: conceptualization, data curation, formal analysis, funding acquisition, investigation (device construction, acoustic experiments, cell culture), methodology, project administration, resources, validation, visualization, writing – original draft, writing – review & editing. Diana Carolina Ochoa: formal analysis, data curation, investigation (cell culture), methodology, validation, visualization, writing – original draft, writing – review & editing. Michael Delay: formal analysis, writing – original draft, writing – review & editing. Itziar González: conceptualization, funding acquisition, investigation (device electrical characterization), methodology, project administration, resources, supervision, visualization, writing – original draft. Marcela Camacho: conceptualization, data curation, formal analysis, investigation (cell culture), methodology, project administration, resources, supervision, visualization, writing – original draft, writing – review & editing.

Conflicts of interest

The authors declare no conflict of interest.

Acknowledgements

This research was supported and funded by the Ministerio de Ciencia, Tecnología e Innovación de Colombia, Minciencias and Centro Internacional de Física, through the postdoctoral position in the Laboratorio de Biofísica, Facultad de Ciencia, Universidad Nacional de Colombia, Sede Bogotá, funded in the Convocatoria 891-2020 (80740-294-2021). We thank Dr Yenny Lozano, Universidad de la Salle, for suggestions in cell culture and Juan Camilo Vargas for assistance with the plotter cut.

Notes and references

1 Y. Fan, X. Wang, J. Ren, F. Lin and J. Wu, *Microsyst. Nanoeng.*, 2022, **8**, 94.
2 R. Joseph, C. Feiyan, F. James, W. Martin and H. Tony Jun, *Nat. Rev. Methods Primers*, 2022, **2**, 30.

3 N. Jakub, L. Andreas and L. Thomas, *Electrophoresis*, 2021, **43**, 804–818.
4 M. Wu, A. Ozcelik, J. Rufo, Z. Wang, R. Fang and T. Jun Huang, *Microsyst. Nanoeng.*, 2019, **5**, 32.
5 L. Fabian, O. Mathias, B. Henrik and O. Pelle, *J. Acoust. Soc. Am.*, 2021, **149**, 4281–4291.
6 G. Icíar, F. Luis José, G. Tomás Enrique, B. Javier, S. Jose Luis and C. Alfredo, *Sens. Actuators, B*, 2010, **144**, 310–317.
7 B. Alireza, M. Peiman, S. Haghjooy Javanmard, S. Sepehrirahnama and A. Sanati-Nezhad, *Sci. Rep.*, 2021, **11**, 22048.
8 V. Jiménez Abelino, C. O. Diana Carolina, D. Michael, G. G. Itziar and C. Marcela, *Ultrasound Med. Biol.*, 2022, **48**, 1202–1214.
9 G. Liu, J. Lei, F. Cheng, L. Kemin, J. Xuanrong, Z. Huang and G. Zhongning, *Micromachines*, 2021, **12**, 876.
10 G. Itziar, R. Rubén Andrés, P. Alberto and C. Pilar, *Micromachines*, 2020, **11**, 751.
11 D. l. Reyes Elena, A. Victor, C. Pilar, P. Alberto and G. Itziar, *J. Acoust. Soc. Am.*, 2021, **150**, 646–656.
12 L. Fabian, O. Mathias, B. Henrik and O. Pelle, *J. Acoust. Soc. Am.*, 2021, **149**, 4281–4291.
13 P. Dow, K. Kotz, S. Gruszka, J. Holder and J. Fiering, *Lab Chip*, 2018, **18**, 923–932.
14 R. P. Moiseyenko and B. Henrik, *Phys. Rev. Appl.*, 2019, **11**, 014014.
15 I. González, J. Earl, L. J. Fernandez, B. Sainz, A. Pinto, R. Monge, S. Alcala, A. Castillejo, J. Soto and A. Carrato, *Micromachines*, 2018, **9**, 129.
16 A. Nastro, M. Baù, M. Ferrari, L. Rufer, S. Basrour and V. Ferrari, *IEEE Sens. J.*, 2024, 1.
17 A. R. Rezk, J. R. Friend and L. Y. Yeo, *Lab Chip*, 2014, **14**, 1802–1805.
18 L. Zhenglong, H. M. Niranjan, S. Kaaliveetil, C. Yu-Hsuan, C. Charmi, P. Veronica, K. M. Amir and B. Sagnik, *Sens. Actuators, B*, 2024, **404**, 135212.
19 I. Gonzalez, I. Navarrete, A. Vargas and M. Camacho, Aluminium-foil chip for ultrasonic particle manipulation, *Acoustofluidics*, Lille, France, 2018.
20 J. Luzuriaga, P. Carreras, M. Candil, D. Bazou and I. González, *Front. Phys.*, 2022, **10**, 920687.
21 K. Worden, *Strain*, 2001, **37**, 167–172.
22 A. Haake and J. Dual, *Ultrasonics*, 2004, **42**, 75–80.
23 H. Albrecht, N. Adrian, K. Deok-Ho, I. Jong-Eun, S. Yu, D. Jürg and J. Byeong-Kwon, *Ultrasound Med. Biol.*, 2005, **31**, 857–864.
24 J. Dual, P. Hahn, I. Leibacher, D. Möller and T. Schwarz, *Lab Chip*, 2012, **12**, 852–862.
25 A. Boskovic, K. M. Jones, A. Velasquez, I. P. Hardy, M. L. Bulos, R. C. Ashley and M. Wiklund, *Am. J. Phys.*, 2024, **92**, 59–64.
26 Q. Wang, M. R. Bentley and S. Oliver, *J. Phys. Chem. C*, 2017, **121**, 14120–14127.
27 Y. Wei, T. Wang, Y. Wang, S. Zeng, Y.-P. Ho and H.-P. Ho, *Micromachines*, 2023, **14**, 656.
28 L. Yao, S. ZhuanZhuan, Y. Ling and M. L. Chang, *RSC Adv.*, 2016, **6**, 85468–85472.
29 Y. Ling and Z. S. Zhuan, *Lab Chip*, 2015, **15**, 1642–1645.
30 H. Wang, Z. Liu, D. M. Shin, Z. G. Chen, Y. Cho, Y.-J. Kim and A. Han, *Microfluid. Nanofluid.*, 2018, **22**, 68.
31 K. G. Fiona, L. C. Ross, F. C. Alan, M. Narla and M. C. Brian, *Blood*, 2002, **99**, 1060–1063.
32 K. Marketa, H. Bettina, H. Jakob, F. Julia, H. Martin, G. Jochen and K. Martin, *Biophys. J.*, 2021, **120**, 2838–2847.